Orientational alignment in Cavity Quantum Electrodynamics

Jonathan Keeling* and Peter G. Kirton
SUPA, School of Physics and Astronomy, University of St Andrews, St Andrews, KY16 9SS, United Kingdom
(Dated: May 9, 2018)

We consider the orientational alignment of dipoles due to strong matter-light coupling, for a non-vanishing density of excitations. We compare various approaches to this problem in the limit of large numbers of emitters, and show that direct Monte Carlo integration, mean-field theory, and large deviation methods match exactly in this limit. All three results show that orientational alignment develops in the presence of a macroscopically occupied polariton mode, and that the dipoles asymptotically approach perfect alignment in the limit of high density or low temperature.

I. INTRODUCTION

When light couples to matter strongly enough, it can change material properties. This general idea has recently seen an explosion of interest across a variety of materials and for a range of physical phenomena, as reviewed briefly below. The most dramatic such effects occur when matter-light coupling induces a phase transition, leading to changes of material properties. Phase transitions occur in the thermodynamic limit, and so rely on understanding matter-light coupling with large numbers of particles. It is therefore important to test approximate theoretical methods that describe matter-light coupling in this limit. Here we provide a comparison of two such methods, mean-field theory and large deviation approaches, in the context of orientational ordering of dipoles coupled to light.

One context in which changes to material properties due to matter-light coupling have been extensively studied is that of organic molecules, which already have interesting photophysics and chemistry even without strong coupling [1–3]. In particular, the possibility to manipulate chemical reaction rates, or allow photocatalysis of multiple reactions by a single photon [4–10] has been studied in such materials. Similarly, the idea of modifying electrical transport [11–13] by strong coupling to a cavity has also been explored. Another developing area is in using strong coupling to affect singlet fission [14], potentially improving solar cell performance. There have also been many works exploring whether the configuration, vibrational state, or orientation of a molecule can be affected by strong coupling to light [7, 15–20], and how strong matter-light coupling may lead to the breakdown of the Born-Oppenheimer approximation [17, 21, 22]. Recently, there have been several reviews discussing these developments, see for example [19, 23–25].

In other contexts, strong driving by external light has been used as a way to induce transient superconductivity [26, 27], with a variety of proposed mechanisms [28–32]. Superconductivity can also be affected by strong matter-light coupling of phonon modes to an infra-red cavity mode [33], or using multimode Terahertz cavities to induce cavity-mediated electron pairing [34]. Similarly structural phase transitions in Perovskites have been found to be modified by strong coupling [35]. In the context of organic molecules, strong coupling between infra-red cavities and vibrational modes has also been studied [16, 36–40].

For many of the above effects, a particularly interesting feature is the possibility of collective effects — i.e. effects of there being many molecules coupled to the same cavity mode. To understand such collective effects, it is necessary to consider the behavior in the limit of a large number, N, of emitters. While for small N it is possible to consider exact numerical methods, such as adapting density functional theory to include cavity QED [41], such exact approaches are challenging for macroscopic numbers of emitters. A number of different theoretical frameworks have been used for tackling these problems. These include using symmetries to reduce the problem size, and mean-field theories [6, 42–45]. From the context of condensed matter physics, mean-field theory is a natural approach. For N emitters coupled to a single mode, mean-field theory is expected to become exact as $N \to \infty$, with corrections scaling as $1/N$. We have shown elsewhere [45] how the absorption spectra of vibrationally dressed molecules can indeed be recovered by such an approach. Here we consider other forms of dressing, and the comparison between mean-field theory and exact numerical methods.

In this article, we focus on the question, first discussed by Cortese *et al.* [44], of how a strong coupling can lead to orientational alignment of molecular dipoles. We compare various approaches to answering this question, using mean-field theory [46, 47], direct Monte-Carlo integration, and large deviation approaches [48]. We find that in the limit of large N, these results all agree (when considering parameter values for which agreement can be expected). We also show the versatility of mean-field approaches to include saturation effects expected at high excitation density. In an appendix, we also show how these methods can be easily adapted to a wider set of related models.

* jmjk@st-andrews.ac.uk

II. MODEL AND SUMMARY OF PREVIOUS RESULTS

We consider a model of N orientable dipoles, strongly coupled to a single cavity mode. Such a model was introduced previously in Refs. 18 and 44. The electronic states of the dipoles are modeled as two-level systems, corresponding to ground and first excited electronic states. Such a description is appropriate when the dipole has an anharmonic spectrum, and this first electronic transition dominates the optical response. The electronic state is thus described by Pauli matrices σ_i and the cavity mode by the creation operator $a^\dagger$. The coupling strength of a dipole, depends on its orientation relative to the electric field direction (we assume a single polarization for simplicity). For dipoles free to rotate in two dimensions we parameterize this by a single alignment angle, θ_i. This leads to the generalized Dicke model [49]:

$$H = \omega a^\dagger a + \sum_i g\cos(\theta_i)(a^\dagger \sigma_i^- + a\sigma_i^+) + \frac{\omega_0}{2}\sigma_i^z. \quad (1)$$

The polariton splitting emerging from such a model scales as $g\sqrt{N}$, so in the following we assume $g\sqrt{N}$ is intensive and so remains finite in the limit of large N. Physically, this scaling occurs because the matter-light coupling g in Eq. (1) scales as $1/\sqrt{V}$ where V is the quantization volume, so $g\sqrt{N}$ scales as the square root of the density of dipoles, an intensive quantity.

Such a model may be considered as describing the orientation of organic molecules in solution, with strong coupling to an optical cavity mode. We note that strong coupling between organic molecules and infra-red cavities has also been studied, however in such a case the electromagnetic mode couples to the displacement of a vibrational mode of the molecule [16, 36–40]. The model in Eq. (1), involving transitions of two-level systems, specifically describes coupling to electronic transitions, not vibrational modes, so we focus only on strong coupling to optical cavities. Closely related models can arise in other contexts. For example, there is a close connection to a model considered in the context of cold atoms in an optical cavity [50], where a Raman process between cavity light and external pump can cause a change of spin state of the atoms, $\sigma_i^\pm$; in this case θ_i denotes the position of the atom in a standing wave of light. Similar models can also be realized in arrays of superconducting qubits [51].

As Eq. (1) is a modified version of the Dicke model [49], such a model can naturally be expected to undergo a version of the Dicke-Hepp-Lieb phase transition [46]. This has been extensively studied in the absence of an orientational degree of freedom, i.e. setting $\theta_i = 0$. In particular, if one considers Eq. (1) in the grand canonical ensemble, with a chemical potential μ controlling the number of excitations $M = a^\dagger a + \sum_i(\sigma_i^z + 1)/2$, there is a transition at low temperatures or high densities to a state where there is a macroscopic occupation of the photon mode [47]. We will discuss further below how this transition is modified by the orientational degree of freedom.

In Cortese *et al.* [44], the behavior of angular orientation following from Eq. (1) in the M excitation sector ground state. i.e., the evolution of $\langle\cos^2\theta\rangle$ as a function of density, M/N and temperature was studied. For reference, we summarize these results here. Focusing on the resonant case, $\omega_0 = \omega$, we may approximately write the energy of the M polariton states as $\epsilon_M \simeq -Mg\sqrt{\sum_i \cos^2\theta_i}$, which leads to an effective partition function:

$$\mathcal{Z} = \prod_i \int d\theta_i \exp\left(\beta M g\sqrt{\sum_i \cos^2\theta_i}\right). \quad (2)$$

This expression neglects any saturation of the polariton splitting at finite excitation density, i.e. it assumes the energy to create M excitations is exactly M times the energy to create one excitation. This is not true for the model in Eq. (1) because the two-level systems are saturable. However, such effects were shown in [44] to not significantly change the behavior. (We also consider this further below.)

The integrals over θ_i can be transformed to an integral over the end-to-end distribution of a polymer. Specifically, we consider

$$\mathbf{R} \equiv \begin{pmatrix} R_x \\ R_y \end{pmatrix} = \sum_i \begin{pmatrix} \cos 2\theta_i \\ \sin 2\theta_i \end{pmatrix},$$

which is the vector formed by adding unit vectors each oriented at angle $2\theta_i$. Then, using $\sum_i \cos^2\theta_i = \sum_i(1 + \cos(2\theta_i))/2 = (N + R_x)/2$, the integral can be rewritten as

$$\mathcal{Z} = \int d\mathbf{R} P_N(\mathbf{R}) \exp\left(Na\sqrt{\frac{1 + R_x/N}{2}}\right)$$

where $a = \beta(M/N)g\sqrt{N}$ and $P_N(\mathbf{R})$ is the probability distribution of the vector $\mathbf{R}$, which can be considered as a polymer chain of N links. The peak of this probability distribution is at $\mathbf{R} = 0$, corresponding to entirely disordered dipoles, and the variance of this distribution scales as $\langle\mathbf{R}^2\rangle \propto N$ as expected for a random walk.

In writing the exponent above, we have explicitly separated the scaling with system size N, from the intensive quantity a which depends on the excitation *density* M/N and the quantity $g\sqrt{N}$ which, as discussed above, remains finite in the limit of large N. As discussed in [44], for the record polariton splitting of $g\sqrt{N} \simeq 0.5$eV, this quantity would at room temperature correspond to $a \simeq 20(M/N)$. The length R_x can also be used to evaluate an order parameter for the orientational ordering, i.e.

$$\langle\cos^2\theta\rangle = \frac{1 + x}{2}, \qquad x = \left\langle \frac{R_x}{N} \right\rangle.$$

To explore ordering, we are interested in how x evolves with the parameter a.

Under the assumption that one may replace $P_N(\mathbf{R})$ with its large N approximation from the central limit theorem, $P_N(\mathbf{R}) \simeq \exp(-R^2/N)/(\pi N)$, one could evaluate the partition function. (However, as discussed further below, this approximation has limited validity). Due to the large parameter N, one may use a saddle point evaluation, leading the to statement that x is given by the minimum of $x^2 - a\sqrt{(1+x)/2}$, given by:

$$a = 4x_0\sqrt{2(1+x_0)} \tag{3}$$

The solution of this equation increases from $x_0 = 0$ at $a = 0$ to reach $x_0 = 1$ when $a = 8$. By definition, $|x_0| < 1$, and so this Gaussian polymer approximation predicts that at $a = 8$, a second order transition occurs to a fully ordered state [44].

III. MEAN-FIELD THEORY OF ORIENTATIONAL ORDERING

In this section we discuss an alternate approach to finding the partition function of Eq. (1): mean-field theory, as has been discussed many times for variants of the Dicke model [46, 47, 52, 53]. As discussed above, we consider the grand canonical ensemble, so the effective Hamiltonian becomes $H - \mu M$. In making comparison to Ref. 44, we will tune the excitation density by adjusting μ. Within mean-field theory, there is a transition between a normal state, with zero photon number, and a condensed state. Mean-field theory proceeds by assuming a coherent state $|\alpha\rangle$ for the photons, and performing a variational minimization over the coherent field amplitude. In the normal state, the minimum occurs at $\alpha = 0$, while for the condensed state, the minimum occurs at finite α. Such an approach can be rigorously justified by evaluating a path integral form of the partition function, and noting that in the limit $N \to \infty$, a saddle point expression becomes exact [47]. Such a procedure implies $\mathcal{Z} = \exp(-\beta F)$ where:

$$F = \inf_{\alpha} \left[(\omega - \mu)|\alpha|^2 - N k_B T \ln\left(\mathrm{Tr} e^{-\beta h}\right) \right], \tag{4}$$

with h being the Hamiltonian of a single dipole in the presence of the coherent field, α:

$$h = \frac{1}{2}\begin{pmatrix} \omega_0 - \mu & 2g\cos\theta_i \alpha^* \\ 2g\cos\theta_i \alpha & -(\omega_0 - \mu) \end{pmatrix}.$$

The trace appearing in the partition function involves both a trace over two by two matrices, as well as a trace over angular orientations.

One can rewrite the above in terms of only intensive quantities by noting the photon density $|\alpha|^2$ scales with N in the condensed state [46], and so writing $|\alpha|^2 = N\rho$. One then finds

$$\frac{F}{N} = \inf_{\rho > 0} \left[(\omega - \mu)\rho - k_B T \ln \mathcal{Z}_{\mathrm{2LS}} \right], \tag{5}$$

$$\mathcal{Z}_{\mathrm{2LS}} = \int d\theta \; 2\cosh\left(\frac{\beta E(\theta)}{2}\right), \tag{6}$$

where we have used the two-level system energy:

$$E(\theta) = \sqrt{(\omega_0 - \mu)^2 + 4(g\sqrt{N})^2 \rho \cos^2\theta}.$$

Once ρ is known, the angular orientation can be found as

$$\langle \cos^2\theta \rangle = \frac{1}{\mathcal{Z}_{\mathrm{2LS}}} \int d\theta \cos^2(\theta) \; 2\cosh\left(\frac{\beta E(\theta)}{2}\right). \tag{7}$$

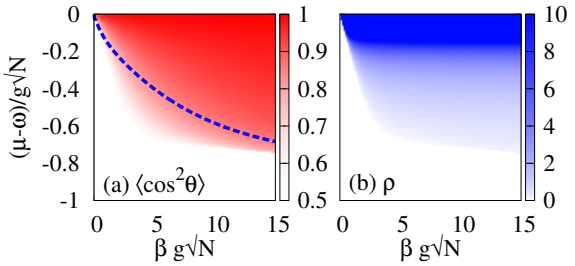

FIG. 1. Mean-field theory results. Panel (a) shows orientational ordering, $\langle \cos^2\theta \rangle$, while panel (b) shows the corresponding condensate density ρ. The dashed line in panel (a) corresponds to the prediction in Ref. 44 for complete ordering, $\beta g\sqrt{N}(M/N) = 8$.

If we focus on the resonant case, $\omega = \omega_0$, the ordering parameter depends on two dimensionless quantities, $\beta g\sqrt{N}$ and $(\mu - \omega)/g\sqrt{N}$. Figure 1 shows the orientational ordering and condensate density as a function of these quantities. When the condensate density is zero, we see immediately from Eq. (7) that $\langle \cos^2\theta \rangle = 0.5$, as the energy $E(\theta)$ becomes independent of θ when $\rho = 0$. Inside the condensed region the orientational order grows and approaches 1. However, crucially we see that it grows smoothly without any sharp transition.

For direct comparison the results of Cortese *et al.* [44], Eq. (3), we must extract the total excitation number, by considering the derivative of free energy with chemical potential:

$$\frac{M}{N} = \rho + \frac{1}{\mathcal{Z}_{\mathrm{2LS}}} \int d\theta \left[1 + \frac{\mu}{E(\theta)}\right] \cosh\left(\frac{\beta E}{2}\right). \tag{8}$$

The trajectory at $a \equiv \beta(M/N)g\sqrt{N} = 8$ is marked by the blue dashed line in Fig. 1. We see this does not correspond to any sharp transition of the orientational ordering.

IV. MONTE CARLO INTEGRATION

Having seen that the mean-field approach predicts no complete orientational ordering at any finite occupation

or temperature, we next compare this to exact numerics at finite N. Specifically, we consider the problem as defined in Eq. (2), and the corresponding orientational ordering quantified by:

$$\langle \cos^2\theta \rangle = \frac{1}{\mathcal{Z}} \prod_i \int d\theta_i \overline{\cos^2\theta} \exp\left(Na\sqrt{\overline{\cos^2\theta}} \right). \quad (9)$$

where we have denoted $\overline{\cos^2\theta} \equiv \sum_i \cos^2\theta_i/N$. This expression may be evaluated directly by Monte Carlo integration. Specifically, we sample configurations $\{\theta_i\}$, and evaluate the expectation of the order parameter $\overline{\cos^2\theta}$ weighted by the Boltzmann factor $P_{\rm Boltz} = \exp\left(Na\sqrt{\overline{\cos^2\theta}} \right)$. To sample this efficiently, we draw samples from a Gaussian approximation of the Boltzmann distribution, i.e. $P_{\rm draw}(\{\theta_i\}) = \prod_i \exp\left(-a\theta_i^2/2\right)$, and weight samples by the ratio $P_{\rm Boltz}/P_{\rm draw}$. The distribution $P_{\rm draw}$ is factorizable, hence it is easy to draw samples from this distribution. In addition $P_{\rm Boltz} \simeq P_{\rm draw}$ for small angles; at low temperature only small angles are probable, so the sampling becomes efficient in this limit. We may also note that in this limit, with independent θ_i, this problem is self averaging, so the sampling error reduces at large N.

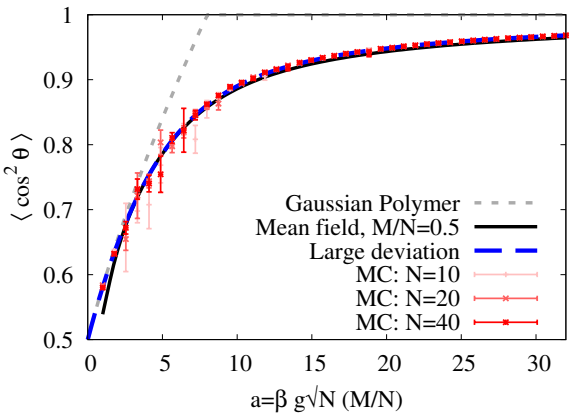

FIG. 2. Order parameter as a function of $a = \beta g\sqrt{N}(M/N)$, comparing Monte Carlo results to mean-field and Gaussian polymer results. Monte Carlo results are shown as points, with error bars reflecting the sampling error, with each point using 20000 samples. The gray short dashed line indicates the Gaussian Polymer prediction [44], $(1 + x_0)/2$ with x_0 given by Eq. (3). The black line shows mean-field prediction in the low temperature, low excitation limit as discussed in the text. The blue long dashed line shows the large deviation result.

The order parameter calculated by this Monte Carlo approach is shown in Fig. 2, for various values of N, in each case choosing excitation fraction $M/N = 0.5$. We clearly see that while the results have converged with respect to N (indeed, even $N = 10$ seems converged), they do not converge on the result of the polymer model described in Sec. II. .

In order to compare these exact numerics to mean-field theory, we must make a number of modifications to the mean-field equations. These follow from the fact that Eq. (2) and the results following from it (a) assume a thermal population of only the lower polariton mode, and (b) neglect saturation effects arising from the nonlinearity of two-level systems. To address point (a), we restrict to the lower energy branch, modifying the mean-field theory by writing $\mathcal{Z}_{\rm 2LS} = \int d\theta e^{\beta E(\theta)/2}$ in contrast to Eq. (6). Such a replacement is valid if $\beta g\sqrt{N} \gg 1$. To address point (b), we work at low excitation fraction $M/N = 0.5$. In the limit $M/N \to 0$, the excitation of each two-level system is small, and so the saturation at a maximum of one excitation per dipole has little effect. One may note that the low temperature and low excitation limits are consistent: if $M/N \ll 1$, then $\beta g\sqrt{N} \gg 1$ for all non-zero a. To fix the excitation fraction M/N, we use Eq. (8) with the replacement $\cosh(\beta E/2) \to \exp(\beta E/2)$ as a self consistent equation to fix μ.

V. LARGE DEVIATIONS

We next turn to consider whether the Polymer model discussed in Cortese *et al.* [44] can be improved to match the behavior seen from the above Monte Carlo results. The approximation which leads to the mismatch is the replacing of $P_N(\mathbf{R})$ by a Gaussian distribution. The reason this approximation fails can be understood as follows: The Gaussian distribution is valid for "typical" values of $\mathbf{R}$, which, means $|\mathbf{R}| \simeq \mathcal{O}(\sqrt{N})$. However, in the limit of large a, the matter-light coupling biases one towards atypical configurations, where $R_x \simeq \mathcal{O}(N)$. Such values are deep in the tail of the probability distribution; they correspond to large deviations from the mean, and are not given by the Gaussian approximation. In fact, in the limit $N \to \infty$, any non-zero value of $x = R_x/N$ corresponds to a large deviation.

A. Analytic large deviation formulation

Fortunately, there is simple approach to extract the probability of large deviations, as reviewed, e.g., by Touchette [48]. We are interested in finding the probability $P_N(x = R_x/N)$ and so we use the standard results of the large deviation formulation:

$$P_N(x) \simeq e^{-Nw(x)}, \quad w(x) = \sup_s \left[xs - \lambda(s) \right], \quad (10)$$

where $\lambda(s)$ is the generating function at large N:

$$\lambda(s) = \lim_{N\to\infty} \left[\frac{1}{N} \ln\langle e^{sR_x} \rangle \right]. \quad (11)$$

This can be directly evaluated for a model of an N link polymer chain,

$$\langle e^{sR_x} \rangle = \prod_i \int d\theta_i \exp\left[s \sum_i \cos(\theta_i) \right] = \left[I_0(s) \right]^N,$$

where $I_0(s)$ is the modified Bessel function of the first kind. Thus, we have:

$$w(x) = \sup_s \left[xs - \ln(I_0(s))\right]. \tag{12}$$

This function $w(x)$ replaces the quadratic exponent in the Gaussian polymer approximation. We can then use this to find an alternative to Eq. (3) for determining x_0. In terms of x, the partition function can be written as:

$$\mathcal{Z} \propto \int dx \exp\left(-Nw(x) + Na\sqrt{\frac{1+x}{2}}\right),$$

and it is clear that at large N, this can be approximated by its saddle point, x_0, given by solving:

$$\left.\frac{dw}{dx}\right|_{x_0} = \frac{a}{2\sqrt{2(1+x_0)}}.$$

To evaluate $w(x)$, we note that the supremum over s in Eq. (12) is solved by $s_0(x)$ such that:

$$x = \left.\frac{d}{ds}\ln I_0(s)\right|_{s=s_0(x)} = \frac{I_1(s_0(x))}{I_0(s_0(x))}.$$

We may then use this to evaluate the derivative of $w(x)$, writing:

$$\frac{dw(x)}{dx} = \frac{\partial w(x)}{\partial x} + \frac{\partial w(x)}{\partial s_0}\frac{ds_0}{dx} = s_0(x).$$

In the final expression we used the explicit form of $w(x)$ to evaluate the first term, and the fact that the second term vanishes by the definition of s_0. Putting these together we find that x_0 is determined by the pair of equations:

$$s_0 = \frac{a}{2\sqrt{2(1+x_0)}}, \qquad x_0 = \frac{I_1(s_0)}{I_0(s_0)}. \tag{13}$$

Solving these simultaneous equations gives the blue long dashed line in Fig. 2 which almost perfectly matches the Monte Carlo result. One may also explicitly see this expression predicts perfect orientation only at zero temperature, i.e., as $a \to \infty$. Assuming $x_0 \simeq 1$ one finds $s_0 \simeq a/4$, giving an explicit expression for x_0 which approaches one asymptotically from below.

B. Recovering large deviation result from mean-field theory

The mean-field theory results at low excitation and low temperature appear to match both the large deviation analytic form and the Monte Carlo results well. Here we show that this match can in fact be seen analytically, by considering the mean-field equations perturbatively in the limit $M/N \to 0$. Crucially, since the expression for M/N in Eq. (8) contains a term ρ, the limit of low density requires that we consider ρ small. In this limit we may expand

$$E(\theta) \simeq |\omega_0 - \mu| + \frac{2\rho g^2 N \cos^2\theta}{|\omega_0 - \mu|}.$$

Using this expansion, combined with the restriction to the lower branch in evaluating $\mathcal{Z}_{\rm 2LS}$, we find that the density equation becomes:

$$\begin{aligned}\frac{M}{N} &= \rho + \frac{1}{\mathcal{Z}_{\rm 2LS}}\int d\theta \frac{g^2 N\rho\cos^2(\theta)}{|\omega_0-\mu|^2} e^{\beta E(\theta)/2} \\ &= \rho\left(1 + \frac{g^2 N\langle\cos^2(\theta)\rangle}{|\omega_0-\mu|^2}\right)\end{aligned} \tag{14}$$

The angular average also simplifies, as we can write

$$E(\theta) \simeq E_0 + E_1\cos(2\theta)$$

which allows angular integrals to be rewritten in terms of modified Bessel functions, namely

$$\langle\cos^2\theta\rangle = \frac{1+x}{2}, \qquad x = \frac{I_1(\beta E_1/2)}{I_0(\beta E_1/2)} \tag{15}$$

where $E_1 = \rho g^2 N/|\omega_0 - \mu|$. We can then combine this with the self-consistency condition, from evaluating the infinum in Eq. (5) which gives:

$$\begin{aligned}(\omega-\mu) &= \frac{1}{\mathcal{Z}_{\rm 2LS}}\int d\theta \frac{1}{2}\frac{dE(\theta)}{d\rho} e^{\beta E(\theta)/2} \\ &\simeq \frac{g^2 N\langle\cos^2(\theta)\rangle}{|\omega_0-\mu|}\end{aligned} \tag{16}$$

In the resonant limit $\omega = \omega_0$, assuming that $\omega > \mu$ as is required for physical solutions, we then find that $\omega - \mu = g\sqrt{N}\sqrt{\langle\cos^2(\theta)\rangle}$, and thus $\rho = M/2N$. Inserting this into the definition of E_1 we find:

$$\frac{\beta E_1}{2} = \frac{\beta(M/N)g\sqrt{N}}{2\sqrt{2(1+x)}} = \frac{a}{2\sqrt{2(1+x)}} \tag{17}$$

Together, Eq. (15,17) precisely recover the large deviation result, hence the agreement of mean-field theory in this limit.

VI. SATURATION EFFECTS

As noted earlier, the polymer model and Monte Carlo results above use the approximation that the energy of an M polariton state, ϵ_M is equal to M times the one polariton state, $\epsilon_M \simeq M\epsilon_1$. Such an assumption is incorrect for Eq. (1), as this model is not linear — it involves saturable two-level systems. In this section we discuss how our results change when we take this saturation and non-linearity into account.

In contrast to the Monte Carlo results and polymer model, the mean-field approach makes no assumption of

linearity. i.e., the mean-field theory is based on solving the exact energies of two-level atoms in the presence of a coherent field. Thus, for the mean-field approach we can directly determine the effect of saturation by considering the behavior at different filling fractions M/N. This is shown in the solid lines in Fig. 3 which show the mean-field results for the orientational ordering. Each line corresponds to a different excitation fraction, and the horizontal axis is the variable $a = \beta g\sqrt{N}(M/N)$, which we may still tune by adjusting $\beta g\sqrt{N}$. We see that the lines do not fall on top of each other, indicating that the results depend on the values M/N and $\beta g\sqrt{N}$ separately — there is no reduction to a single result depending only on $a = \beta g\sqrt{N}(M/N)$. This indicates an effect of saturation, as it means we no longer can match the large deviation result, as we could in the limit $M/N \to 0$.

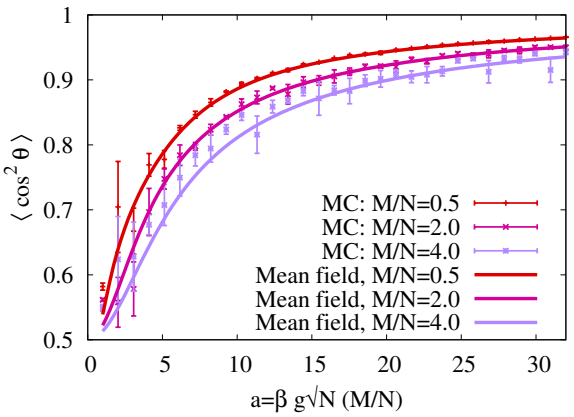

FIG. 3. Comparison of mean-field theory results at various excitation fractions to Monte Carlo calculations allowing for saturation effects. Excitation fraction increases from top ($M/N = 0.5$) to bottom ($M/N = 4.0$). The Monte Carlo results correspond to $N = 10$ molecules; each point is calculated with 4000 samples.

Next, we consider how to modify the Monte Carlo integration to recover correct results at a finite excitation density. As noted above, the error in the polymer model comes by assuming $\epsilon_M(\{\theta_i\}) \simeq M\epsilon_1(\{\theta_i\} \equiv -Mg\sqrt{\sum_i \cos^2\theta_i}$. To correct this, we must therefore replace Eq. (2) with

$$\mathcal{Z} = \prod_i \int d\theta_i \exp\left(-\beta\epsilon_M(\{\theta_i\})\right), \tag{18}$$

using the true energy of the M excitation state of Eq. (1). We find this energy numerically: For each configuration of angles $\{\theta_i\}$ we construct the Hamiltonian in the M excitation subspace, find its lowest eigenvalue, and use this value as $\epsilon_M(\{\theta_i\})$. For $M \geq N$, this requires us to find the lowest eigenvalue of a 2^N dimensional matrix for each configuration $\{\theta_i\}$; when $M < N$ the matrix size can be smaller. For $N = 10$, we thus require eigenvalues of a 1024×1024 matrix for each configuration, this is achievable, but computationally costly so we take only 4000 samples. The results of this are also shown as the data points in Fig. 3. There is reasonable agreement between the mean-field and $N = 10$ Monte Carlo results for $M/N = 0.5$ and $M/N = 2.0$; the agreement is less clear at the highest excitation level; this is likely due to the finite size effects for $N = 10$.

VII. SUMMARY

In this article we have shown that the evolution of orientational order with temperature and density can be captured both through a large deviation formula, and through mean-field theory. The large deviation approach is derived from an approximate partition function valid in the low excitation density limit. In this limit mean-field theory exactly reproduces the large deviation approach. Furthermore, we have shown that away from this limit, mean-field theory matches exact numerics well, indicating the validity of mean-field theory for general excitation densities. The behavior we find shows a smooth evolution of ordering with excitation and temperature, and does not undergo any sharp transition to a fully ordered state.

An important conclusion of this work is that mean-field theory can indeed be used as a simple and adaptable theoretical tool to understand a variety of other related models. i.e., one may replace rotational orientation with a variety of ways of dressing the Dicke model such as deformation of a molecule or vibrational state etc. The case of vibrational dressing using this mean-field approach was already considered in Ref. 53.

The validity of mean-field theory for such problems is also useful in that mean-field approaches can be easily adapted to non-equilibrium situations. An extension to the non-equilibrium version of this problem would be an interesting challenge for future work, exploring how incoherent excitation balanced with cavity loss can potentially lead to a modification of orientational ordering. Another related extension involves considering multiple polarizations of light, and the relation between orientational order and the polarization of the condensate. This can potentially form a "strong coupling" analogue to recent discussions of the polarization state in a weak coupling photon BEC [54, 55].

ACKNOWLEDGMENTS

We are grateful to S. De Liberato for useful discussions. JK and PGK acknowledges financial support from EPSRC program "Hybrid Polaritonics" (EP/M025330/1).

Appendix A: Three dimensional orientation

The approach outlined above allows simple extensions to other models. For example, we can consider dipoles

allowed to rotate in three dimensions, by considering

$$\mathcal{Z} = \prod_i \int d\theta_i \sin(\theta_i) \int d\phi_i \exp\left(\beta M g \sqrt{\sum_i \cos^2\theta_i}\right). \tag{A1}$$

The ϕ integral is of course trivial here (as we have chosen the electric field to be aligned along the z axis). The θ integral is modified by the changed integral measure.

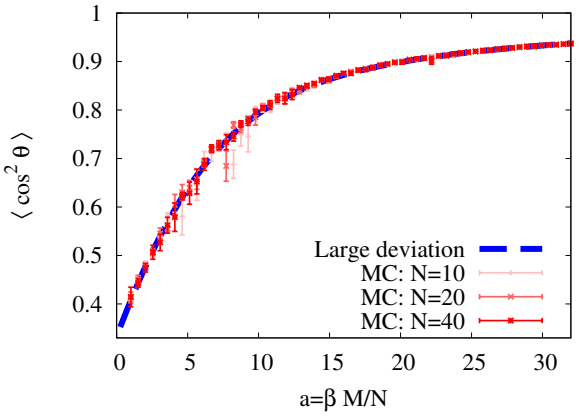

FIG. 4. Comparison of Monte Carlo using the one-excitation state, and large deviation results for rotational orientation of three dimensional dipoles. Lines are as in Fig. 2; data correspond to 2000 samples for each point.

The large deviation approach remains applicable, in terms of the variable $x = \sum_i \cos(2\theta_i)/N$. The generating function $\lambda(s)$ now takes a different form, namely:

$$\lambda(s) = -s - \frac{1}{2}\ln(s) + \ln\left[\mathrm{Erfi}(\sqrt{2s})\right] + \text{const.}.$$

From this expression, we then find the self consistent equations for x_0, s_0 take the form:

$$s_0 = \frac{a}{2\sqrt{2(1+x_0)}}, \tag{A2}$$

$$x_0 = -1 - \frac{1}{2s_0} + \sqrt{\frac{2}{\pi s_0}}\frac{e^{2s_0}}{\mathrm{Erfi}(\sqrt{2s_0})}. \tag{A3}$$

Figure 4 shows these results, again comparing to Monte Carlo integration of Eq. (A1). Once again, at large a the results asymptotically approach complete alignment, but without any sharp transition. The behavior at small a differs from the previous case: at infinite temperatures, the angular average now gives $\langle\cos^2\theta\rangle = 1/3$ rather than $1/2$.

As well as the large deviation formula, mean-field theory can also be directly applied to this problem. This corresponds to replacing the integral over angle θ in Eq. (6) by:

$$\mathcal{Z}_{\mathrm{2LS}} = \int d\theta \sin(\theta) \int d\phi 2\cosh\left(\frac{\beta E(\theta)}{2}\right).$$

It is once again possible to show that the mean-field result, in the limits $M/N \to 0$ and $\beta g\sqrt{N} \gg 1$, recovers the same form as the large deviation expression.

[1] V. M. Agranovich, *The Theory of Excitons* (Nauka, Moscow, 1968).
[2] V. M. Agranovich, *Excitations in Organic Solids* (Oxford University Press, Oxford, 2009).
[3] W. Barford, *Electronic and optical properties of conjugated polymers* (Oxford University Press, Oxford, 2013).
[4] T. Schwartz, J. A. Hutchison, C. Genet, and T. W. Ebbesen, Phys. Rev. Lett. **106**, 196405 (2011).
[5] J. A. Hutchison, T. Schwartz, C. Genet, E. Devaux, and T. W. Ebbesen, Ang. Chem. Int. Ed. **51**, 1592 (2012).
[6] F. Herrera and F. C. Spano, Phys. Rev. Lett. **116**, 238301 (2016).
[7] J. Galego, F. J. Garcia-Vidal, and J. Feist, Nat. Commun. **7**, 13841 (2016).
[8] M. Kowalewski, K. Bennett, and S. Mukamel, J. Phys. Chem. Lett. **7**, 2050 (2016).
[9] J. Flick, M. Ruggenthaler, H. Appel, and A. Rubio, Proc. Natl. Acad. Sci. **114**, 3026 (2017).
[10] J. Galego, F. J. Garcia-Vidal, and J. Feist, "Many-Molecule Reaction Triggered by a Single Photon in Polaritonic Chemistry," (2017).
[11] E. Orgiu, J. George, J. A. Hutchison, E. Devaux, J. F. Dayen, B. Doudin, F. Stellacci, C. Genet, J. Schachenmayer, C. Genes, G. Pupillo, P. Samorì, and T. W. Ebbesen, Nat. Mater. **14**, 1123 (2015).
[12] J. Feist and F. J. Garcia-Vidal, Phys. Rev. Lett. **114**, 196402 (2015).
[13] D. Hagenmüller, S. Schütz, J. Schachenmayer, C. Genes, and G. Pupillo, (2018), arXiv:1801.09876.
[14] L. A. Martnez-Martnez, M. Du, R. F. Ribeiro, S. Kna-Cohen, and J. Yuen-Zhou, The Journal of Physical Chemistry Letters **9**, 1951 (2018).
[15] A. Canaguier-Durand, E. Devaux, J. George, Y. Pang, J. A. Hutchison, T. Schwartz, C. Genet, N. Wilhelms, J.-M. Lehn, and T. W. Ebbesen, Angew. Chemie Int. Ed. **52**, 10533 (2013).
[16] A. Shalabney, J. George, J. Hutchison, G. Pupillo, C. Genet, and T. W. Ebbesen, Nat. Comm. **6**, 5981 (2015).
[17] J. Galego, F. J. Garcia-Vidal, and J. Feist, Phys. Rev. X **5**, 41022 (2015).
[18] J. A. Ćwik, P. Kirton, S. De Liberato, and J. Keeling, Phys. Rev. A **93**, 033840 (2016).
[19] J. Feist, J. Galego, and F. J. Garcia-Vidal, ACS Photonics **5**, 205 (2018).
[20] L. A. Martínez-Martínez, R. F. Ribeiro, J. Campos-González-Angulo, and J. Yuen-Zhou, ACS Photonics **5**, 167 (2018).
[21] K. Bennett, M. Kowalewski, and S. Mukamel, Faraday Discuss. **194**, 259 (2016).

[22] J. Flick, H. Appel, M. Ruggenthaler, and A. Rubio, J. Chem. Theory Comput. **13**, 1616 (2017).
[23] F. Herrera and F. C. Spano, ACS Photonics **5**, 65 (2018).
[24] B. Kolaric, B. Maes, K. Clays, T. Durt, and Y. Caudano, (2018), arXiv:1802.06029.
[25] R. F. Ribeiro, L. A. Martínez-Martínez, M. Du, J. Campos-Gonzalez-Angulo, and J. Yuen-Zhou, (2018), arXiv:1802.08681.
[26] D. Fausti, R. I. Tobey, N. Dean, S. Kaiser, A. Dienst, M. C. Hoffmann, S. Pyon, T. Takayama, H. Takagi, and A. Cavalleri, Science **331**, 189 (2011).
[27] M. Mitrano, A. Cantaluppi, D. Nicoletti, S. Kaiser, A. Perucchi, S. Lupi, P. Di Pietro, D. Pontiroli, M. Riccò, S. R. Clark, D. Jaksch, and A. Cavalleri, Nature **530**, 461 (2016).
[28] R. Mankowsky, A. Subedi, M. Först, S. O. Mariager, M. Chollet, H. T. Lemke, J. S. Robinson, J. M. Glownia, M. P. Minitti, A. Frano, M. Fechner, N. A. Spaldin, T. Loew, B. Keimer, A. Georges, and A. Cavalleri, Nature **516**, 71 (2014).
[29] M. Knap, M. Babadi, G. Refael, I. Martin, and E. Demler, Phys. Rev. B **94**, 214504 (2016).
[30] D. M. Kennes, E. Y. Wilner, D. R. Reichman, and A. J. Millis, Nat. Phys. **13**, 479 (2017).
[31] M. A. Sentef, A. Tokuno, A. Georges, and C. Kollath, Phys. Rev. Lett. **118**, 087002 (2017).
[32] F. Schlawin, A. S. D. Dietrich, M. Kiffner, A. Cavalleri, and D. Jaksch, Phys. Rev. B **96**, 064526 (2017).
[33] M. A. Sentef, M. Ruggenthaler, and A. Rubio, (2018), arXiv:1802.09437.
[34] F. Schlawin, A. Cavalleri, and D. Jaksch, (2018).
[35] S. Wang, A. Mika, J. A. Hutchison, C. Genet, A. Jouaiti, M. W. Hosseini, and T. W. Ebbesen, Nanoscale **6**, 7243 (2014).
[36] J. George, A. Shalabney, J. A. Hutchison, C. Genet, and T. W. Ebbesen, J. Phys. Chem. Lett. **6**, 1027 (2015).
[37] J. del Pino, J. Feist, and F. J. Garcia-Vidal, New J. Phys. **17**, 53040 (2015).
[38] A. Shalabney, J. George, H. Hiura, J. a. Hutchison, C. Genet, P. Hellwig, T. W. Ebbesen, P. Hellwig, and T. W. Ebbesen, Ang. Chem. Int. Ed. **54**, 7971 (2015).
[39] J. del Pino, J. Feist, and F. J. Garcia-Vidal, J. Phys. Chem. C **119**, 29132 (2015).
[40] A. Strashko and J. Keeling, Phys. Rev. A **94**, 023843 (2016).
[41] J. Flick, C. Schafer, M. Ruggenthaler, H. Appel, and A. Rubio, ACS photonics **5**, 992 (2018).
[42] F. Herrera and F. C. Spano, Phys. Rev. Lett. **118**, 223601 (2017).
[43] F. Herrera and F. C. Spano, Phys. Rev. A **95**, 053867 (2017).
[44] E. Cortese, P. G. Lagoudakis, and S. De Liberato, Phys. Rev. Lett. **119**, 043604 (2017).
[45] M. A. Zeb, P. G. Kirton, and J. Keeling, ACS Photonics **5**, 249 (2018).
[46] Y. K. Wang and F. T. Hioe, Phys. Rev. A **7**, 831 (1973).
[47] P. R. Eastham and P. B. Littlewood, Phys. Rev. B **64**, 235101 (2001).
[48] H. Touchette, Phys. Rep. **478**, 1 (2009).
[49] B. M. Garraway, Phil. Trans. R. Soc. A **369**, 1137 (2011).
[50] F. Mivehvar, F. Piazza, and H. Ritsch, Phys. Rev. Lett. **119**, 063602 (2017).
[51] K. Kakuyanagi, Y. Matsuzaki, C. Déprez, H. Toida, K. Semba, H. Yamaguchi, W. J. Munro, and S. Saito, Phys. Rev. Lett. **117**, 210503 (2016).
[52] F. M. Marchetti, J. Keeling, M. H. Szymańska, and P. B. Littlewood, Phys. Rev. B **76**, 115326 (2007).
[53] J. A. Ćwik, S. Reja, P. B. Littlewood, and J. Keeling, Eur. Lett. **105**, 47009 (2014).
[54] R. I. Moodie, P. Kirton, and J. Keeling, Phys. Rev. A **96**, 043844 (2017).
[55] S. Greveling, F. van der Laan, H. C. Jagers, and D. van Oosten, (2017), arXiv:1712.08426.